

# Mode-locking in driven vortex lattices with transverse ac-drive and random pinning

Alejandro B. Kolton<sup>1</sup>, Daniel Domínguez<sup>1</sup>, and Niels Grønbech-Jensen<sup>2,3</sup>

<sup>1</sup>Centro Atómico Bariloche and Instituto Balseiro, 8400 S. C. de Bariloche, Río Negro, Argentina

<sup>2</sup>Department of Applied Science, University of California, Davis, California 95616

<sup>3</sup>NERSC, Lawrence Berkeley National Laboratory, Berkeley, California 94720

(February 1, 2008)

We find mode-locking steps in simulated current-voltage characteristics of driven vortex lattices with *random* pinning when an applied ac-current is *perpendicular* to the dc-current. For low frequencies there is mode-locking only above a non-zero threshold ac force amplitude, while for large frequencies there is mode-locking for any small ac force. This is consistent with the nature of *transverse* temporal order in the different regimes in the absence of an applied ac-drive. For large frequencies the magnitude of the fundamental mode-locked step depends linearly with the ac force amplitude.

PACS numbers: 74.60.Ge, 74.40.+k, 05.70.Fh

Non-linear dynamics of vortices driven by a current in random media leads to several interesting non-equilibrium phases, such as plastic flow, moving smectic and moving Bragg glass.<sup>1-7</sup> These dynamical phases can be characterized by their temporal order<sup>2,4,7-9</sup> and mode-locking responses.<sup>10-12</sup> When a vortex array with average intervortex spacing  $a$  is moving at a high enough velocity  $v$ , it is possible to have temporal order at the washboard frequency  $\omega_0 = 2\pi v/a$ , which results in a peak at  $\omega_0$  in the voltage power spectrum.<sup>8,9</sup> This has been observed in numerical simulations<sup>4,12</sup> and also recently in experiments.<sup>8,9</sup> When the system is driven by a dc + ac force with frequency  $\Omega$ , interference phenomena leads to mode-locking steps for vortex velocities such that  $\omega_0 = (p/q)\Omega$ .<sup>10-12</sup> This interesting effect has been observed experimentally by Fiory<sup>10</sup> and by Harris *et al.*<sup>11</sup> Recently, we have numerically studied how the existence of mode-locking in driven vortex lattices depends on the presence of temporal order in each dynamical regime.<sup>12</sup>

Mode-locking phenomena has been extensively studied in other systems in the past, e.g., Josephson junctions (Shapiro steps),<sup>13</sup> Josephson junction arrays,<sup>14</sup> superconductors with periodic pinning<sup>15-17</sup> and charge density waves (CDW).<sup>19,20</sup> Driven vortex lattices with random pinning have two important features that distinguish them from these systems. (i) There is no inherent periodicity, as for example in Josephson junction arrays and superconductors with periodic pinning. Temporal order and periodicity are induced dynamically due to the vortex-vortex interaction, which tends to favor a structure close to a triangular vortex lattice at large velocities.<sup>2</sup> (ii) The vortex displacements are two-dimensional vectors. This is an important difference with respect to CDW systems where the displacement field is a scalar.<sup>20</sup> In particular, the behavior of the displacements in the direction perpendicular to the driving force shows phenomena like a transverse critical current<sup>2,4,6</sup> and a transverse freezing transition<sup>2,5</sup> at high velocities. It can therefore be interesting to study the possibility of mode-locking when an ac force is applied in the direction *perpendicular* to the direction of the dc driving force. Recently, it has been found in rectangular periodic pin-

ning arrays<sup>17</sup> and in Josephson junction arrays<sup>18</sup> that a transverse ac force leads to a new type of “transverse” phase-locking in these cases. In this paper we will investigate the possibility of *transverse mode-locking* in driven vortices with random pinning.

The dynamics of a vortex in position  $\mathbf{r}_i$  is given by:<sup>4,5</sup>

$$\eta \frac{d\mathbf{r}_i}{dt} = - \sum_{j \neq i} \nabla_i U_v(r_{ij}) - \sum_p \nabla_i U_p(r_{ip}) + \mathbf{F}(t), \quad (1)$$

where  $r_{ij} = |\mathbf{r}_i - \mathbf{r}_j|$  is the distance between vortices  $i, j$ ,  $r_{ip} = |\mathbf{r}_i - \mathbf{r}_p|$  is the distance between the vortex  $i$  and a pinning site at  $\mathbf{r}_p$ ,  $\eta = \frac{\Phi_0 H_{c2} d}{c^2 \rho_n}$  is the Bardeen-Stephen friction and  $\mathbf{F}(t) = \frac{d\Phi_0}{c} [\mathbf{J}_{dc} + \mathbf{J}_{ac} \cos(\Omega t)] \times \mathbf{z}$  is the driving force due to an alternating current  $\mathbf{J}_{ac} \cos(\Omega t)$  superimposed to a constant current  $\mathbf{J}_{dc}$ . The vortex-vortex interaction is considered logarithmic:  $U_v(r) = -A_v \ln(r/\Lambda)$ , with  $A_v = \Phi_0^2/8\pi\Lambda$ , and  $\Lambda = 2\lambda^2/d$  is the effective penetration depth of a thin film of thickness  $d$ .<sup>5,12</sup> The vortices interact with a random distribution of attractive pinning centers with  $U_p(r) = -A_p e^{-(r/\xi)^2}$ ,  $\xi$  being the coherence length. Length is normalized by  $\xi$ , energy by  $A_v$ , and time by  $\tau = \eta \xi^2/A_v$ . We consider  $N_v$  vortices and  $N_p$  pinning centers in a rectangular box of size  $L_x \times L_y$ , and the normalized vortex density is  $n_v = N_v \xi^2/L_x L_y = B \xi^2/\Phi_0$ . Moving vortices induce a total electric field  $\mathbf{E} = \frac{B}{c} \mathbf{v} \times \mathbf{z}$ , with  $\mathbf{v} = \frac{1}{N_v} \sum_i \mathbf{v}_i$ .

We study the response of the vortex lattice to a dc force plus a *transverse* ac force,  $\mathbf{F} = F_{dc} \mathbf{y} + F_{ac} \cos(\Omega t) \mathbf{x}$  solving Eq. (1) for different values of  $F_{ac}$  and  $\Omega$ . The simulations are at  $T = 0$  for a vortex density  $n_v = 0.04$  in a box with  $L_x/L_y = \sqrt{3}/2$ , and  $N_v = 64, 100, 144, 196, 256, 400$  (we show results for  $N_v = 256$ ), and we consider weak pinning strength of  $A_p/A_v = 0.05$  with a density of pinning centers being  $n_p = 0.08$ . We impose periodic boundary conditions and the long-range interaction is determined by Ref. 21. The time integration step is  $\Delta t = 0.001\tau$  and averages are evaluated during 131072 steps after 3000 steps for equilibration.

In a previous work<sup>12</sup> we studied the case of a longitudinal ac force, relating the mode-locking response with the

presence of temporal order for the longitudinal component of the velocity. Here we analyze now the *transverse temporal order* from the transverse power voltage spectra (corresponding to the transverse velocity), which are

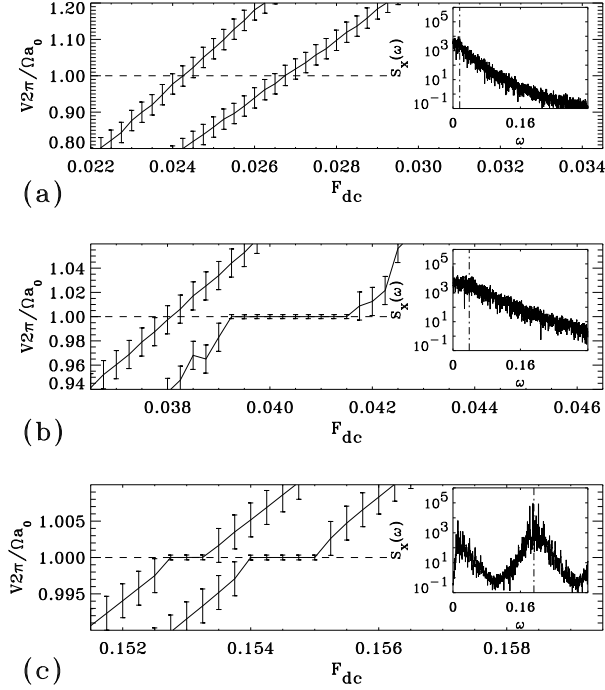


FIG. 1. Velocity-force curve around the main interference condition  $V = \Omega a_0/2\pi$  for three typical drive frequencies  $\Omega$ . Each case show results for two values of amplitude  $F_{ac}$  (the curves are shifted in  $F_{dc}$  for clarity). Insets show corresponding voltage power spectrum for  $F_{ac} = 0$  and  $V \approx V_{step}$ . Vertical dashed line in the spectral density indicates the expected washboard frequency  $\omega_0$ . (a)  $\Omega = 0.02$ ,  $F_{ac} = 0.01$  (left),  $F_{ac} = 0.03$  (right). (b)  $\Omega = 0.04$ ,  $F_{ac} = 0.02$  (left),  $F_{ac} = 0.08$  (right). (c)  $\Omega = 0.19$ ,  $F_{ac} = 0.09$  (left),  $F_{ac} = 0.23$  (right).

shown in the insets of Fig. 1. They are calculated as  $S_x(\omega) = |\frac{1}{T} \int_0^T dt V_x(t) \exp(i\omega t)|^2$  at the different dynamical regimes for  $F_{ac} = 0$ .<sup>5</sup> The first regime above the critical depinning force  $F_c$  is the plastic flow regime ( $F_c < F_{dc} < F_p$ ,  $F_c \approx 0.01$ ,  $F_p \approx 0.03$ ). In this case we find a broad band spectrum without temporal order [inset of Fig. 1(a)]. Similar behavior is found in the “smectic flow” regime ( $F_p < F_{dc} < F_t$ ,  $F_t \approx 0.06$ ), shown in the inset of Fig. 1(b). This is reasonable, since we know that the transverse motion is diffusive in both regimes.<sup>5</sup> Only for  $F_{dc} > F_t$ , in the “transverse solid” regime, we find clear evidence of temporal order in the transverse velocity. This is seen in the inset of Fig. 1(c) where well developed peaks appear at the washboard frequency,  $\omega_0$ , and its harmonics. We are now ready to study the response to a superimposed transverse ac-force  $F_{ac} \cos(\Omega t)$ , for varying values of  $F_{ac}$ . For a given  $\Omega$ , we expect the main interference step ( $p = q = 1$ ) to occur when  $V = V_{step} = \Omega a/2\pi$  (i.e.,  $\Omega = \omega_0$ ) if there

is mode-locking. We therefore choose the values of  $\Omega$  such that the expected step,  $V_{step} = \Omega a/2\pi$ , would correspond to velocities  $V$  belonging to a given dynamical regime of the limit  $F_{ac} = 0$ . Each simulation is started at  $\langle v_y \rangle \approx 0.975\Omega a/2\pi$  with an ordered triangular

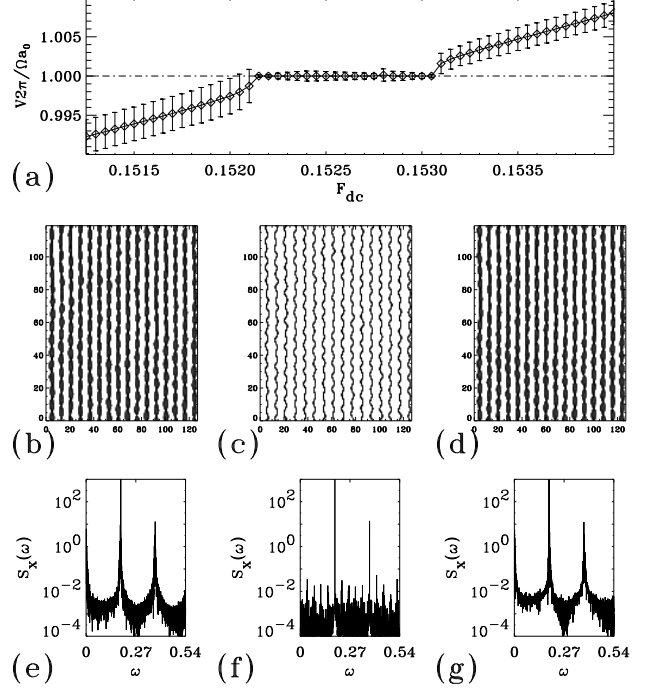


FIG. 2. (a) Velocity-force curve around the main interference step for  $\Omega = 0.08$  and  $F_{ac} = 0.3$ . (b)-(c)-(d) Typical time averaged coarse-grained density of vortices for a mode-unlocked state below the step, a mode-locked state in the step, and a mode-unlocked state above the step, respectively. (e) Typical voltage power spectrum for the three ac-driven regimes mentioned above.

lattice up to values such that  $\langle v_y \rangle \approx 1.025\Omega a/2\pi$  by slowly increasing the dc force  $F_{dc}$  with  $\Delta F_{dc} = 0.00005 - 0.00025$ . For low  $\Omega$ , for which we have plastic flow when  $F_{ac} \rightarrow 0$ , we find that there are no interference steps in a wide range of  $F_{ac}$  (shown in Fig. 1(a) for  $F_{ac}/V_{step} < 1$  (left curve) and  $F_{ac}/V_{step} > 1$  (right curve)). For intermediate  $\Omega$ , for which we have smectic flow when  $F_{ac} \rightarrow 0$ , we find that there are no steps for small amplitudes,  $F_{ac}/V_{step} < 1$ , while there are steps for  $F_{ac}/V_{step} > 1$ , as shown in Fig. 1(b) in the left and right curves, respectively. For high  $\Omega$ , corresponding to a transverse solid regime when  $F_{ac} \rightarrow 0$  we find that there are steps both for small  $F_{ac}/V_{step} < 1$  and large  $F_{ac}/V_{step} > 1$  values of the ac amplitude, as we can observe in Fig. 1(c). We therefore find a behavior similar to the case of longitudinal ac forces.<sup>12</sup> In the present case, when the dynamical regime has transverse temporal order, any small amount of  $F_{ac}$  will induce transverse mode-locking, while for the dynamical regimes that do not have transverse temporal order, a non-zero (threshold) value of  $F_{ac}$  is needed to

induce transverse mode-locking.

In Fig. 2(a) we show in detail a typical  $V - F_{dc}$  curve around the transverse mode-locking step. To visualize the spatial structure of trajectories in the transition we define a coarse-grained vortex density  $\rho_v(\mathbf{r}, t)$ . We take a coarse-graining scale  $\Delta r < a_0$ . In Fig. 2(b)-(c)-(d) we

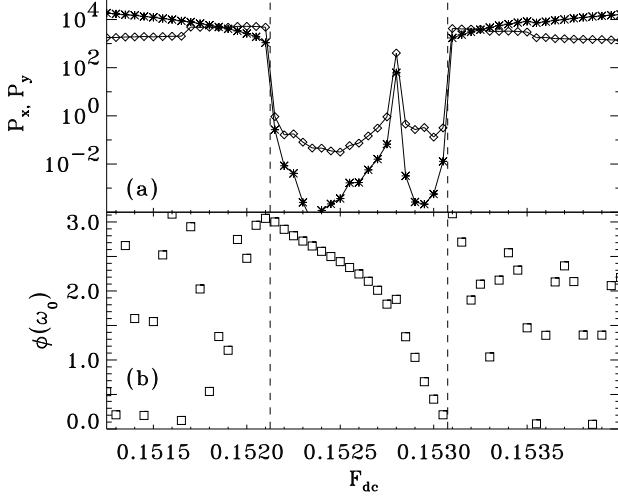


FIG. 3. (a) Low frequency voltage noise in the transverse and longitudinal direction around the main interference step. The dashed lines indicate the mode-locking transitions. (b) Phase of the washboard frequency component of the longitudinal voltage Fourier transform around the step.

show the temporal average  $\langle \rho_v(\mathbf{r}, t) \rangle$  of the density for three typical values of  $F_{dc}$ , corresponding to voltages  $V < V_{step}$  (Fig. 2(b)),  $V = V_{step}$  (Fig. 2(c)), and  $V > V_{step}$  (Fig. 2(d)). We observe in Fig. 2(b) that within the mode-locked state vortices follow one-dimensional trajectories. The wavy nature of the trajectories is, of course, due to the transverse ac force. Figures 2(e)-(f)-(g) show typical transverse voltage spectral densities  $S_x(\omega)$  for the three cases mentioned above. We see that there is a significant reduction in the width of the washboard peak within the step; a typical signature of mode-locking.<sup>19,20</sup> In Fig. 3(a) we show the low frequency voltage noise in both directions, perpendicular  $P_x$  and longitudinal  $P_y$  to the dc-force, defined as  $P_{x,y} = \lim_{\omega \rightarrow 0} S_{x,y}(\omega)$ . We see that also the low frequency noise is greatly reduced within the step. (There is a noise peak inside the step which corresponds to a transition between different mode-locked structures). In Fig. 3(b) we show the phase  $\phi(\omega_0)$  of the washboard frequency component of the longitudinal voltage Fourier transform  $\tilde{V}(\omega_0)$ , defined as  $\tilde{V}(\omega_0) = \sqrt{S_y(\omega_0)} \exp(i\phi(\omega_0))$ . Here we see explicitly that within the “phase-locked” state there is a well defined “phase” which varies within the range  $0 \leq \phi \leq \pi$ .

In Fig. 4(a-b) we show the range (width)  $\Delta F_{dc}$  for the case  $F_p < F_{dc} < F_t$  and  $F_t < F_{dc}$  respectively. The error bars and the mean values were estimated by repeating

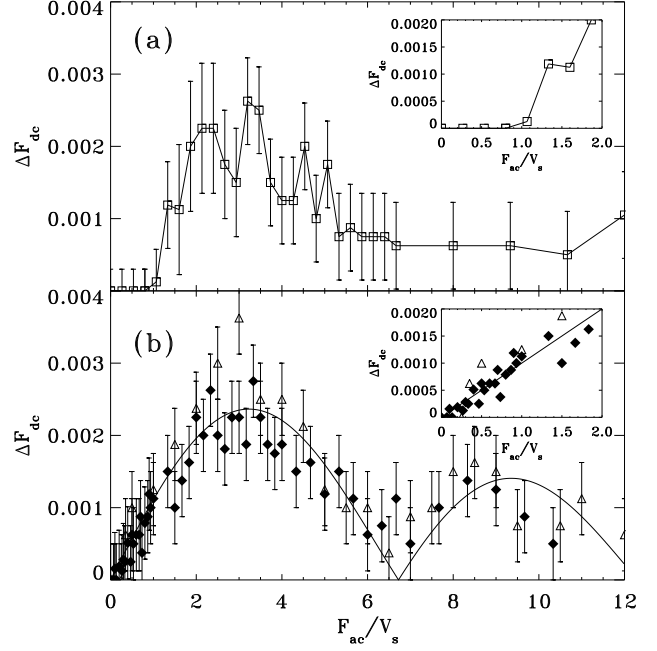


FIG. 4. Step width  $\Delta F_{dc}$  vs  $F_{ac} 2\pi / \Omega a_0 = F_{ac} / V_{step}$ . (a)  $\Omega = 0.04$ . (b)  $\Omega = 0.13$  ( $\triangle$ ) points and  $\Omega = 0.19$  ( $\diamond$ ) points. Solid line shows a fit to  $A |J_1(F_{ac} / V_{step} \sqrt{3})|$ .

the simulation for three different disorder realizations. In Fig. 4(a) we show  $\Delta F_{dc}$  for  $\Omega = 0.04$  vs  $F_{ac}$ , which corresponds to the smectic flow regime for  $F_{ac} \rightarrow 0$ . We see that there is mode-locking only above a non-zero threshold value  $F_{ac} / V_{step} \approx 1$  (see inset of Fig. 1(a)). In Fig. 4(b) we show  $\Delta F_{dc}$  for two frequencies  $\Omega = 0.13, 0.19$  vs  $F_{ac}$ , which correspond to the transverse solid in the  $F_{ac} = 0$  limit. We can collapse (approximately) both curves into a single curve if we plot  $\Delta F_{dc}$  vs  $F_{ac} / V_{step}$ . Our results follow closely a dependence of the form  $\Delta F_{dc} \approx A |J_1(F_{ac} / V_{step} \sqrt{3})|$  with  $A$  being a constant. In the inset of Fig. 4(b) we can see that there is a linear dependence of the mode-locking intensity with  $F_{ac}$ . This is very different from transverse mode-locking in periodic pinning systems,<sup>17,18</sup> in which the step width follows  $\Delta F_{dc} \propto (F_{ac})^2$ . The rather surprising result that in the random pinning case the transverse mode-locking intensity has a linear  $F_{ac}$ -dependence can be explained as a consequence of the existence of transverse temporal order in the  $F_{ac} = 0$  limit. We can show this with a very simple effective model. The moving lattice can be described approximately by an equation of motion for the velocity  $\mathbf{v}$  of its center of mass,

$$\mathbf{v} = \mathbf{F}_{dc} + \mathbf{F}_{ac} \cos(\Omega t) - \sum_{\mathbf{G}} \mathbf{G} U_{\mathbf{G}} \sin(\mathbf{G} \cdot \mathbf{r}). \quad (2)$$

The  $U_{\mathbf{G}}$  are the components of an effective periodic force, due to the interaction of the nearly periodic moving lattice (with reciprocal vectors  $\mathbf{G}$ ) with disorder. For weak disorder (small  $U_{\mathbf{G}}$ ) a first order correction can be ob-

tained assuming that in zero order  $\mathbf{r} = \mathbf{r}_0 + \langle \mathbf{v} \rangle t + \mathbf{F}_{ac} \sin(\Omega t)/\Omega$ . This gives for the instantaneous velocity  $\mathbf{v}$  and average velocity  $\langle \mathbf{v} \rangle$  the following expressions at first order in  $F_{ac}$ :

$$\mathbf{v} = \mathbf{F}_{dc} - \sum_{\mathbf{G}} \mathbf{G} U_{\mathbf{G}} \sin \left[ \mathbf{G} \cdot (\mathbf{r}_0 + \langle \mathbf{v} \rangle t) \right] \left[ J_0 \left( \frac{\mathbf{G} \cdot \mathbf{F}_{ac}}{\Omega} \right) + 2J_1 \left( \frac{\mathbf{G} \cdot \mathbf{F}_{ac}}{\Omega} \right) \sin(\Omega t) \right] \quad (3)$$

$$\langle \mathbf{v} \rangle = \mathbf{F}_{dc} - \sum_{\mathbf{G}} \mathbf{G} U_{\mathbf{G}} \sin(\mathbf{G} \cdot \mathbf{r}_0) \left\{ J_0 \left( \frac{\mathbf{G} \cdot \mathbf{F}_{ac}}{\Omega} \right) \delta(\mathbf{G} \cdot \langle \mathbf{v} \rangle) - 2J_1 \left( \frac{\mathbf{G} \cdot \mathbf{F}_{ac}}{\Omega} \right) \delta(\mathbf{G} \cdot \langle \mathbf{v} \rangle - \Omega) \right\} \quad (4)$$

We consider now an anisotropic triangular lattice with one of its principal axes parallel to  $\mathbf{F}_{dc} = \mathbf{y} F_{dc}$ , and for simplicity we keep only the shortest reciprocal vectors  $\{\mathbf{G}\} = \{\mathbf{g}_s, \mathbf{g}_l, \mathbf{g}_l - \mathbf{g}_s\}$  where  $\mathbf{g}_s = \mathbf{x} \frac{2\pi}{a_0} \frac{2}{\sqrt{3}}$  and  $\mathbf{g}_l = \mathbf{x} \frac{2\pi}{a_0} \frac{1}{\sqrt{3}} + \mathbf{y} \frac{2\pi}{a_0}$ . Then, we consider  $U_{\mathbf{g}_l} = U_l = U_{\mathbf{g}_l - \mathbf{g}_s} + \Delta U_l$  and  $U_{\mathbf{g}_s} = U_s$ . Here  $\Delta U_l$  represents a small deformation of the perfect triangular lattice in the  $\mathbf{y}$  direction.  $U_s$  and  $U_l$  could be related, respectively, to the smectic and longitudinal structure factor peaks of the moving vortex system. For  $\mathbf{F}_{ac} = F_{ac} \mathbf{x}$  we obtain for the transverse velocity in the limit  $F_{ac} = 0$ ,

$$v_x = -\frac{2\pi \Delta U_l}{a_0 \sqrt{3}} \sin \left[ \frac{2\pi}{a_0} (r_0 + \langle v \rangle t) \right]. \quad (5)$$

With this approach we obtain the phase-locking range for the first interference step  $\Omega = \omega_0$ ,

$$\Delta F_{dc} = \frac{4\pi |\Delta U_l|}{a_0} |J_1 \left( \frac{\mathbf{g}_l \cdot \mathbf{F}_{ac}}{\Omega} \right)| = \frac{4\pi |\Delta U_l|}{a_0} \left| J_1 \left( \frac{F_{ac}}{V_{step} \sqrt{3}} \right) \right|. \quad (6)$$

Even when it was derived for small  $F_{ac}$  and small disorder, Eq. (6) is the approximate relation found in the simulation, shown in Fig. 4(b). From equations (5) and (6) we see that, for small  $F_{ac}$ , temporal order in the transverse direction is directly related through  $\Delta U_l$  with the linear dependence of  $\Delta F_{dc}$  on  $F_{ac}$ . It is interesting to note that in the perfectly periodic case,  $\Delta U_l = 0$ , there is no “transverse temporal order” and the mode-locked step widths would be quadratic in  $F_{ac}$ . This is because in the periodic case vortices would move in straight lines without any transverse component of the velocity, and transverse mode-locking would arise as a second order effect. In conclusion, a small amount of disorder (random pinning) is enough to induce transverse temporal order, and, thus, a linear step width dependence with  $F_{ac}$ .

We acknowledge discussions with V. I. Marconi and C. Reichhardt. This work has been supported by CONICET, CNEA and ANPCYT (Argentina) and by the Director, Office of Adv. Sci. Comp. Res., Div. of Math.

Inf. and Comp. Sci. of the U.S.D.O.E. (contract DE-AC03-76SF00098).

- 
- <sup>1</sup> H. J. Jensen *et al.*, Phys. Rev. Lett. **60**, 1676 (1988); A.-C. Shi and A. J. Berlinsky, *ibid.* **67**, 1926 (1991).
  - <sup>2</sup> A. E. Koshelev and V. M. Vinokur, Phys. Rev. Lett. **73**, 3580 (1994); S. Scheidl and V. M. Vinokur, Phys. Rev. B **57**, 13800 (1998); T. Giamarchi and P. Le Doussal, Phys. Rev. Lett. **76**, 3408 (1996); P. Le Doussal and T. Giamarchi, Phys. Rev. B **57**, 11356 (1998); L. Balents, M. C. Marchetti and L. Radzihovsky, *ibid.* **57**, 7705 (1998).
  - <sup>3</sup> F. Pardo *et al.*, Nature **396**, 348 (1998).
  - <sup>4</sup> K. Moon *et al.*, Phys. Rev. Lett. **77**, 2778 (1996); S. Ryu *et al.*, *ibid.* **77**, 5114 (1996); N. Grønbech-Jensen *et al.*, *ibid.* **76**, 2985 (1996); C. Reichhardt *et al.*, *ibid.* **78**, 2648 (1997); D. Domínguez *et al.*, *ibid.* **78**, 2644 (1997); C. J. Olson *et al.*, *ibid.* **81**, 3757 (1998); D. Domínguez, *ibid.* **82**, 181 (1999); H. Fangohr *et al.*, Phys. Rev. B **63**, 064505 (2001); K. Bassler *et al.*, *ibid.* **64**, 224517 (2001).
  - <sup>5</sup> A. B. Kolton *et al.*, Phys. Rev. Lett. **83**, 3061 (1999); Phys. Rev. B **62**, R14657 (2000).
  - <sup>6</sup> C. J. Olson and C. Reichhardt, Phys. Rev. B **61**, R3811 (2000); H. Fangohr *et al.*, *ibid.* **63**, 064501 (2001).
  - <sup>7</sup> L. Balents and M. P. A. Fisher, Phys. Rev. Lett. **75**, 4270 (1995).
  - <sup>8</sup> A. M. Troyanovski *et al.*, Nature **399**, 665 (1999).
  - <sup>9</sup> Y. Togawa *et al.*, Phys. Rev. Lett. **85**, 3716 (2000).
  - <sup>10</sup> A. T. Fiory, Phys. Rev. Lett. **27**, 501 (1971); Phys. Rev. B **7**, 1881 (1973); Phys. Rev. B **8**, 5039 (1973).
  - <sup>11</sup> J. M. Harris *et al.*, Phys. Rev. Lett. **74**, 3684 (1994).
  - <sup>12</sup> A. B. Kolton *et al.*, Phys. Rev. Lett. **86**, 4112 (2001).
  - <sup>13</sup> S. Shapiro, Phys. Rev. Lett. **11**, 80 (1963); A. Barone and G. Paterno, *Physics and Applications of the Josephson Effect* (Wiley, New York, 1982).
  - <sup>14</sup> S. Benz *et al.*, Phys. Rev. Lett. **64**, 693 (1990); K. H. Lee *et al.*, *ibid.* **64**, 692 (1990); D. Domínguez and J.V. Jose, Phys. Rev. Lett. **69**, 514 (1992); Int. J. Mod. Phys. B **8**, 3749 (1994).
  - <sup>15</sup> P. Martinoli *et al.*, Solid State Commun. **17**, 207 (1975); L. Van. Look *et al.*, Phys. Rev. B **60**, R6998 (1999).
  - <sup>16</sup> C. Reichhardt *et al.*, Phys. Rev. B **61**, R11914 (2000).
  - <sup>17</sup> C. Reichhardt *et al.*, Phys. Rev. B **64**, 134508 (2001).
  - <sup>18</sup> V. I. Marconi, A. B. Kolton and D. Domínguez, to be published.
  - <sup>19</sup> G. Grüner, Rev. Mod. Phys. **60**, 1129 (1988); S. Bhattacharya *et al.*, Phys. Rev. Lett. **59**, 1849 (1987); M. H. Higgs *et al.*, *ibid.* **70**, 3784 (1993).
  - <sup>20</sup> L. Sneddon *et al.*, Phys. Rev. Lett. **49**, 292 (1982); S. N. Coppersmith and P. B. Littlewood, *ibid.* **57**, 1927 (1986); A. A. Middleton *et al.*, *ibid.* **68**, 1586 (1992).
  - <sup>21</sup> N. Grønbech-Jensen, Int. J. Mod. Phys. C **7**, 873 (1996); Comp. Phys. Comm. **119**, 115 (1999).